

Heavy particles in incompressible flows: the large Stokes number asymptotics

J er mie Bec ^a, Massimo Cencini ^{b,c}, Rafaela Hillerbrand ^{a,d}

^a CNRS UMR 6202, Observatoire de la C te d'Azur, BP4229, 06304 Nice Cedex 4, France

^b CNR, Istituto dei Sistemi Complessi, Via dei Taurini 19, 00185 Roma, Italy

^c INFN-SMC c/o Dip. di Fisica Universit  Roma 1, P.zzle A. Moro 2, 00185 Rome, Italy.

^d Institut f r theoretische Physik, Westf lische Wilhelms-Univ., M nster, Germany.

Abstract

The dynamics of very heavy particles suspended in incompressible flows is studied in the asymptotics in which their response time is much larger than any characteristic time of fluid motion. In this limit of very large Stokes numbers, particles behave as if suspended in a δ -correlated-in-time Gaussian flow. At those spatial scales where the fluid velocity field is smooth, following Piterbarg [SIAM J. Appl. Math. 62 (2001) 777] and Mehlig *et al.* [Phys. Rev. E 72 (2005) 051104], the two-particle dynamics is reduced to a non-linear system of three stochastic differential equations with additive noise. This model is used to single out the mechanisms leading to the preferential concentration of particles. Scaling arguments are used to predict the large Stokes number behavior of the distribution of the stretching rate and of the probability distribution function of the longitudinal velocity difference between two particles. The latter is characterized by power law tails with exponent -3 in two dimensions. This algebraic behavior is a statistical trademark of particles approaching very closely each other. As for the fractal character of the particle distribution, strong numerical evidence is obtained in favor of saturation of the correlation dimension to the space dimension at large Stokes numbers. Numerical results, obtained at large as well as at small and intermediate values of the Stokes number, reveal that this model catches the most significant qualitative features of particle clustering observed in real flows.

Key words: Stochastic flows, Inertial particles, Lyapunov exponents, Preferential concentration

1 Introduction

Dust, impurities, droplets, air bubbles, and other finite-size particles transported by incompressible flows are commonly encountered in many natural phenomena and industrial processes. A salient feature of such suspensions is

the presence of strong inhomogeneities in the spatial distribution of particles. This phenomenon is dubbed ‘preferential concentration’ (see, e.g., [1]). Such inhomogeneities are important in so far as they affect the probability to find particles close to each other. Thus they have influence on their possibility to collide or to interact biologically, chemically, and gravitationally. Examples showing the importance of the phenomenon are rain initiation by droplet coalescence in warm clouds [2–4], coexistence between several species of plankton in the hydrosphere [5,6], or planet formation by dust accretion in the solar system [7,8]. Engineering applications encompass optimization of spray combustion in Diesel engines [9,10] and in rocket propellers [11].

Particles with a finite size and possibly a mass density different from that of the carrier fluid have inertia. They do not evolve as simple point-like fluid tracers and are termed ‘inertial particles’. It can be shown that if their size is below the smallest active scale of the flow (e.g. the Kolmogorov length-scale in turbulent flows), the particles are subject to drag, buoyancy, added mass, lift force, etc. (see, e.g., [12]). Here we are interested in the limit where particles are not only very small, but also much denser than the surrounding fluid. They then interact with the fluid only through a Stokes viscous drag whose characteristic time (made dimensionless by normalizing it with the typical time scale of the carrier flow) is referred to as the ‘Stokes number’ St . Experiments [1,13] and numerical simulations [14–16] show that the degree of inhomogeneity in the spatial distribution of the suspended particles is a non-trivial function of the Stokes number with a maximum at $St \approx 1$.

Quantifying analytically this dependence is an open question. Various attempts have revealed that the tools used in the study of dissipative dynamical systems are well suited for analyzing preferential concentrations at spatial scales where the carrier flow is smooth. More precisely, the inhomogeneous distribution of particles can be traced back to the fact that their dynamics is dissipative. In contrast to tracers in incompressible fluids whose dynamics is conservative, inertial particles have a dissipative dynamics stemming from their friction with the fluid. In the position-velocity phase space, their trajectories converge to a dynamically evolving attracting set which is generically multifractal [17,18]. The particle spatial distribution, obtained by projecting these singular sets onto the physical space, can also be multifractal [19]. Many observables introduced in the framework of dynamical systems, such as correlation dimension, Lyapunov exponents, or stretching rates, bring important information on particle concentration. Little is known about the dependency of these observables on the Stokes number. Several attempts in determining it have been made in simplified settings: small Stokes number asymptotics [20–22], Gaussian flows with finite [23–25,19] and zero correlation time [26–29].

In this paper we focus on inertial particles in the limit of very large Stokes numbers. In Section 2 we show that in this limit, no matter the actual na-

ture of the underlying carrier flow provided it is statistically homogeneous and isotropic, the particles do behave as if suspended in a time-uncorrelated Gaussian flow. This result was derived independently in [30]. The evolution equations of two- particle motion are derived in Section 3 for those spatial scales where the flow can be considered smooth. Following [26] and [28], we show that for the relative motion of two suspended particles it is sufficient to consider a three-dimensional (random) dynamical system. Instead of the full position-velocity phase space, this system involves only the inter-particle distance, the velocity difference parallel to the relative separation and the modulus of the perpendicular velocity component. We relate this reduced dynamics to different observables quantifying inhomogeneities in the particle distribution and provide some heuristic understanding of this model.

In Section 4 we extend the scaling arguments, which were developed in [28] for the Lyapunov exponent, in order to obtain the large Stokes number behavior of the longitudinal velocity distribution and of the distribution of the stretching rate. These predictions are confirmed by numerical simulations. Moreover, numerical experiments reveal algebraic tails with exponent -3 for the probability distribution function (pdf) of the longitudinal velocity difference between two particles. This signals non-trivial statistics for those events in which the particles come very close to each other. However, such scaling arguments give only access to the leading-order behavior at large Stokes numbers. They cannot be used to understand, for instance, the asymptotic behavior of the fractal (correlation) dimension of the particle spatial distribution. This issue is then investigated with the help of numerical simulations in Section 5. In particular, we provide evidence for the saturation of the correlation dimension to the space dimension. To detect such a saturation, a detailed analysis of the particle distribution in the full position-velocity phase space is required, together with a detailed understanding of its projection onto the physical space.

Beside the physical relevance in the large St asymptotics, spatially smooth Gaussian carrier flows without time correlations are valuable models for systematic investigations. For this reason, we analyze in Section 6 the particle distribution for small and intermediate values of the Stokes number. In contrast to the behavior observed in more realistic flows [22,19,21,24], it is observed that for $St \ll 1$ the deviation from a uniform distribution is linear in St . The general qualitative picture is nonetheless in accordance with observations in real flows. In fact, simulations show that deviations from uniformity are strongest at intermediate values of the Stokes number. This indicates that the mechanism leading to the presence of such strong deviations cannot be simply explained phenomenologically using the arguments often found in the literature (see, e.g., [1]). In particular, this cannot be due to an ‘optimal’ response to the correlation time of the flow structures, as a δ -correlated flow has no structures. Section 7 is devoted to concluding remarks and summarizes the main findings. The Appendices provide some details on the numerical methods.

2 Model dynamics at large Stokes numbers

For suspensions that are so dilute that collisions between particles, hydrodynamic interactions among close particles and retro-action of the particles on the flow can be disregarded, the equations governing the evolution of a spherical particle with density ρ different from that of the carrier fluid ρ_f have been derived in [12]. It was assumed there that the particle radius a is much smaller than the Kolmogorov scale η and that the particle Reynolds number is very small. This implies that the flow surrounding the particle can be approximated by a pure Stokes flow.

In the present paper, we consider impurities that are much heavier than the carrier fluid ($\rho \gg \rho_f$) in the absence of gravity. With these assumptions, the time evolution of the particle position $\mathbf{X}(t)$ takes the simple form:

$$\frac{d^2 \mathbf{X}}{dt^2} = -\frac{1}{\tau} \left[\frac{d\mathbf{X}}{dt} - \mathbf{u}(\mathbf{X}(t), t) \right], \quad (1)$$

where $\tau = (2a^2\rho)/(9\nu\rho_f)$ is the particle response time, the so-called ‘Stokes time’, and ν denotes the kinematic viscosity of the carrier fluid.

We are interested in particles with substantial inertia, meaning that $\tau \gg \tau_f$, where τ_f denotes the largest characteristic time of the carrier flow. In a first approximation, such particles relax infinitely slowly to the fluid velocity. Along the particle path, the local structure of the fluid velocity field changes several times in the interval of time τ required for a significant change of the particle velocity. Thus, on the typical time scales of particle motion, the effective fluid velocity field behaves as a time-uncorrelated process. This can be shown formally by rescaling the time as $s = t/\tau$, so that (1) becomes

$$\frac{d^2 \mathbf{X}}{ds^2} = -\frac{d\mathbf{X}}{ds} + \tau \mathbf{u}(\mathbf{X}(\tau s), \tau s). \quad (2)$$

Now, the time correlation of the velocity field τ_f being finite, the central-limit theorem yields

$$\tau^{1/2} u_i(\mathbf{x}, \tau s) \stackrel{\text{law}}{\sim} \tilde{u}_i(\mathbf{x}, s) \quad \text{when } \tau \gg \tau_f,$$

where $\tilde{\mathbf{u}}$ is a δ -correlated Gaussian process. Thus, equation (2) can be equivalently written as

$$\frac{d^2 \mathbf{X}}{ds^2} = -\frac{d\mathbf{X}}{ds} + \tau^{1/2} \tilde{\mathbf{u}}(\mathbf{X}, s).$$

Transforming s back to the physical time t , we finally obtain the following

evolution equation:

$$\frac{d^2 \mathbf{X}}{dt^2} = -\frac{1}{\tau} \left[\frac{d\mathbf{X}}{dt} - \tilde{\mathbf{u}}(\mathbf{X}(t), t) \right]. \quad (3)$$

Hence, particles with very large inertia behave as if suspended in a Gaussian, δ -correlated in time carrier velocity field. In the following, for the sake of notation simplicity, we shall omit the tilde on the fluid velocity and refer to \mathbf{u} as a δ -correlated carrier flow.

In many real flows, the small-scale properties can be understood by considering a spatially smooth, statistically homogeneous and isotropic velocity field. These spatial properties carry over to the limiting procedure leading to approximating the fluid flow by a δ -correlated Gaussian flow. The incompressible fluid velocity field is then defined by the following correlation functions

$$\langle u_i(\mathbf{x}, t) u_j(\mathbf{y}, t') \rangle = D_{ij}(\mathbf{x} - \mathbf{y}) \delta(t - t'),$$

with

$$D_{ij}(\mathbf{r}) = 2D_0 \delta_{ij} - d_{ij}(\mathbf{r}), \quad (4)$$

$$d_{ij}(\mathbf{r}) = D_1 \left((d+1)r^2 \delta_{ij} - 2r_i r_j \right) + o(r^2). \quad (5)$$

where $r = |\mathbf{r}|$ and d is the space dimension. The constants D_0 and D_1 measure the intensity of the velocity fluctuations and of the velocity gradient, respectively. They define two time-scales of the velocity field. Considering particles with very large inertia amounts to assuming that τ is much larger than both of these time scales.

Note that the approximation of the fluid velocity by a δ -correlated noise has been derived independently with more details in [30]. Such velocity fields with zero time correlation belong to the so-called ‘Kraichnan ensemble’ [31]. Such flows have been studied extensively in the last decade in the context of passive scalar transport [32,33]. They are generally much more tractable than other random flows because of the Gaussianity and the δ -correlation in time. In particular, Equation (3) together with (4) and (5) leads to closed equations for particle density correlations in the position-velocity phase space. In spite of such a simplification, a straightforward solution of these equations cannot be obtained by the kind of traditional techniques generally used in studying Fokker-Planck systems.

3 Two-particle dynamics

The main focus in this paper is on the relative motion of two particles. This allows us, for instance, to study dispersion in terms of the exponential separation of particles and of the Lyapunov exponent λ . Two-particle statistics are also important in understanding spatial distribution of particles and so in quantifying their preferential concentrations.

The equation of motion (3) implies that the separation $\mathbf{R} = \mathbf{X}' - \mathbf{X}$ between two particles evolves according to

$$\frac{d^2 \mathbf{R}}{dt^2} = -\frac{1}{\tau} \left(\frac{d\mathbf{R}}{dt} - \delta \mathbf{u} \right), \quad (6)$$

where

$$\delta \mathbf{u} = \mathbf{u}(\mathbf{X}'(t), t) - \mathbf{u}(\mathbf{X}(t), t).$$

For spatially smooth flows, the velocity difference $\delta \mathbf{u}$ can be approximated at small scales by $\boldsymbol{\sigma}(t) \mathbf{R}$, where $\sigma_{ij}(t) = (\partial u_i / \partial x_j)(\mathbf{X}(t), t)$ is the strain matrix along the trajectory $\mathbf{X}(t)$. In the asymptotics of $St \gg 1$, the velocity correlation functions are given by (4)-(5). This implies that $\boldsymbol{\sigma}$ is to leading order a Gaussian random matrix with correlation given by (see, e.g., [33])

$$\langle \sigma_{ij}(t) \sigma_{kl}(t') \rangle = 2\delta(t - t') D_1 [(d + 1)\delta_{ik}\delta_{jl} - \delta_{ij}\delta_{kl} - \delta_{il}\delta_{jk}]. \quad (7)$$

The two-particle dynamics (6) can then be recast in terms of the following system of stochastic differential equations in the position-velocity phase space (\mathbf{R}, \mathbf{V}) :

$$\begin{aligned} d\mathbf{R} &= \mathbf{V} dt, \\ d\mathbf{V} &= -\frac{1}{\tau} \mathbf{V} dt + \frac{1}{\tau} d\boldsymbol{\sigma} \mathbf{R}. \end{aligned} \quad (8)$$

Here and henceforth we make use of the Ito formalism. The linearized system (8) is usually referred to as the tangent-space dynamics in the theory of dynamical systems.

The two-point motion, given by (8) together with the correlation (7), depends on two time scales only: the particle response time τ and the inverse of the typical velocity gradient $1/D_1$. Rescaling the physical time t by one of these two characteristic times, the resulting dynamics depends on a single non-dimensional parameter, the Stokes number $St \equiv D_1 \tau$. To be consistent with the asymptotics of large inertia, we have to consider $St \gg 1$, though the model is well defined for any value of the Stokes number. Notice that in the case of a turbulent carrier flow, D_1^{-1} is typically proportional to τ_η , the eddy turnover

time associated to the Kolmogorov scale η . The large inertia assumptions thus implies $\tau/\tau_\eta \gg 1$.

3.1 Reduced dynamics

In contrast to the case of tracers, the two-point dynamics of inertial particles has to be considered in the full $(2 \times d)$ -dimensional position-velocity phase space. However, in both two and three dimensions, the number of variables necessary to describe the relative motion of two particles can be reduced to three. As shown in [26] and in [28] (see also [29]) for $d = 2$ and for $d = 3$ respectively, it is indeed sufficient to consider the particle distance $R = |\mathbf{R}|$ and the two velocity difference components, namely V_\parallel in the direction of \mathbf{R} and $|\mathbf{V}_\perp|$ in the directions perpendicular to it. The relative velocity is thus decomposed as

$$\mathbf{V} = V_\parallel \hat{\mathbf{R}} + \mathbf{V}_\perp, \quad \text{with} \quad \hat{\mathbf{R}} = \mathbf{R}/|\mathbf{R}|.$$

It is convenient to introduce the non-dimensional velocity differences X and Y defined as

$$X \equiv \frac{\tau}{R} V_\parallel = \frac{\tau}{R^2} \mathbf{R} \cdot \mathbf{V} \quad \text{and} \quad Y \equiv \frac{\tau}{R} |\mathbf{V}_\perp| = \left| \frac{\tau}{R} \mathbf{V} - X \hat{\mathbf{R}} \right|.$$

Then the original $(2 \times d)$ -dimensional dynamics (8) reduces to a closed system of three stochastic differential equations for R , X and Y . In two dimensions, it takes the form

$$dR = X R ds, \tag{9}$$

$$dX = -\left(X + X^2 - Y^2\right) ds + \sqrt{2St} dB_1, \tag{10}$$

$$dY = -\left(Y + 2XY\right) ds + \sqrt{6St} dB_2, \tag{11}$$

where the rescaled time is $s = t/\tau$, $St = D_1\tau$, and B_i 's denote two independent Brownian motions. In three dimensions the equations for R and X are the same, while Y is a solution of

$$dY = -\left(Y + 2XY - \frac{4St}{Y}\right) ds + \sqrt{6St} dB_2. \tag{12}$$

In deriving these Langevin equations, we made use of the specific form (7) for the correlation of the strain matrix $\boldsymbol{\sigma}$. Note that the positivity of Y have to be ensured by supplementing the system with reflective boundary conditions on the plane $Y = 0$.

There are other advantages of the new system (9)–(12) compared to the original one (8), besides the reduction of the number of variables. The noise terms are now additive, while in the original system they depend on the particle relative distance R . The price to pay is that the drift terms are nonlinear, due to the Ito formula applied to the nonlinear transformation $\{\mathbf{R}, \mathbf{V}\} \rightarrow \{R, X, Y\}$. Such drift terms are different in two and three dimensions because of the term $\propto 1/Y$ for $d = 3$. Such a term is actually present in any dimension $d > 2$. It can be interpreted as a geometrical constraint on the reduced dynamics that prevents the velocity difference between the two particles from becoming exactly parallel to their separation (i.e. $Y = 0$). This is a constraint of codimension $d - 1$. In two dimensions, an arbitrary vector that evolves in time generically satisfies it at discrete times. That is why the geometrical constraint is absent and the singular term does not appear.

The difference between two and three dimensions is more apparent than substantial. Indeed, with the change of variables $\{X, Y\} \rightarrow \{X, \mathcal{Y} = Y^2\}$, the reduced equations in both two and three dimensions can be written as

$$\begin{aligned} dX &= -\left(X + X^2 - \mathcal{Y}\right) ds + \sqrt{2St} dB_1, \\ d\mathcal{Y} &= -2\left(\mathcal{Y} + 2X\mathcal{Y} - \alpha_d St\right) ds + 2\sqrt{6St} \mathcal{Y}^{1/2} dB_2, \end{aligned}$$

where $\alpha_{d=2} = 3$ while $\alpha_{d=3} = 7$. This somewhat more compact formulation makes evident that the dynamics are actually very similar. These stochastic differential equations involve a multiplicative noise term. This formulation will not be used in the sequel as it is more convenient to work with the additive noise formulation (9)–(12).

3.2 Statistical characterization of two-point motion

According to (9), the time integral of the non-dimensional longitudinal velocity difference X yields exponential growth of the inter-particle separation R in physical space:

$$R(s) = R(0) \exp\left(\int_0^s X(s') ds'\right). \quad (13)$$

The Oseledets theorem [34] ensures that, under the ergodicity hypothesis on the dynamics, the separation behaves at large times as $R \propto \exp(\lambda t) = \exp(\lambda \tau s)$, λ being the well-known *Lyapunov exponent*.¹ This non-random quantity is an important measure of particle relative motion. For instance, a positive Lyapunov exponent means that the particle dynamics is chaotic [17].

¹ Strictly speaking, λ equals the Lyapunov exponent only in the case of passive tracers. For inertial particles instead, the full phase-space evolution has to be considered. However, for $St \neq 0$, λ is a lower bound to the true Lyapunov exponent.

According to (13), the Lyapunov exponent can be expressed in terms of the reduced variables as

$$\lambda = \lim_{t \rightarrow \infty} \mu(t), \quad \text{where } \mu(t) = \frac{1}{t} \int_0^{t/\tau} X(s') ds'. \quad (14)$$

If the reduced dynamics is ergodic one has $\lambda = \langle X \rangle / \tau$, where the angular brackets denote averages with respect to the realizations of the noises B_1 and B_2 . At large but finite physical time t , the *stretching rate* $\mu(t)$ gets more and more sharply distributed around λ . More precisely, it obeys a large deviation principle and its pdf takes the asymptotic form (see, e.g., [33,35])

$$p(\mu, t) \propto e^{-(t/\tau)H(\tau\mu)} \quad \text{when } t \rightarrow \infty, \quad (15)$$

where H is a convex function attaining its minimum equal to 0 for $\mu = \lambda$. The *rate function* H measures the large fluctuations of μ , which are important to quantify the clustering properties of the particles. Even if the Lyapunov exponent is positive, the finite-time stretching rate can be negative with a non-zero probability. This indicates that, although on average particles separate exponentially, they may spend a long time close to each other — a sign of a non-trivial clustering behavior.

The statistics of the stretching rate gives information on the *separation probability* $P_2(r)$, that is the probability that the distance R between two particles is less than r . This quantity is expected to behave as a power law at small distances:

$$P_2(r) \propto r^{\mathcal{D}_2} \quad \text{as } r \rightarrow 0. \quad (16)$$

The exponent \mathcal{D}_2 is usually referred to as the *correlation dimension* of the spatial distribution of particles [36,37]. When the particles distribute uniformly, \mathcal{D}_2 equals the space dimension d . Discrepancies from a uniform distribution appearing when $\mathcal{D}_2 < d$ are a signal of preferential concentration. The small-separation behavior (16) implies that the *generalized Lyapunov exponent* Λ of order $-\mathcal{D}_2$ vanishes (see, e.g., [35]), i.e.

$$\Lambda(-\mathcal{D}_2) \equiv \lim_{t \rightarrow \infty} \frac{1}{t} \ln \langle [R(t)/R(0)]^{-\mathcal{D}_2} \rangle = 0. \quad (17)$$

From (14), (15) and (17) one obtains that the correlation dimension is related to the rate function of the stretching rate through a Legendre transformation [33]:

$$\min_{\rho} [\mathcal{D}_2 \rho + H(\rho)] = 0. \quad (18)$$

Another useful quantity for characterizing inhomogeneous particle distributions is the *approaching rate* $\kappa(r)$. It is defined as the flux of particles that are separated by a distance less than r and approach each other, i.e. such that

their longitudinal velocity difference $X(t)$ is negative:

$$\kappa(r) = \frac{1}{\tau} \langle R X \theta(-X) \theta(r - R) \rangle , \quad (19)$$

where θ denotes the Heaviside function. As discussed in [25], $\kappa(r)$ can be related to the collision rate among two particles in the framework of the so-called ‘ghost collision scheme’ [25,38]. This approach consists in counting collision events while allowing particles to overlap instead of scattering. This yields a reliable estimation of the collision rate only in extremely diluted suspensions. The time of relaxation of the particle dynamics to a statistically stationary regime is then much faster than the typical time between two successive collisions of one particle. At small separations the approaching rate behaves as a power law (see [25] for details):

$$\kappa(r) \propto r^\gamma \quad \text{as } r \rightarrow 0. \quad (20)$$

All the quantities introduced here, of course, depend on the only parameter of the dynamics, the Stokes number St . Their behavior in the limit $St \gg 1$ will be examined in Section 4 by means of scaling arguments applied to the reduced dynamics.

3.3 Qualitative picture

For two dimensions, the general picture of the drift in the (X, Y) -plane is shown in Fig. 1(a). Neglecting the effects of the gradient of the fluid velocity field (i.e. disregarding the noises in (10) and (11)), we are left with the drift term only. The trajectories followed by the two-particle motion in the (X, Y) -plane are then circles passing by two fixed points. The unstable fixed point at $(-1, 0)$ corresponds to $V_{\parallel} = -R/\tau$, a relation between relative velocity and separation that is conserved by the dynamics. This relation leads to an exponential convergence of the trajectories of different particles to each other in physical space. The stable fixed point at $(0, 0)$ corresponds to a vanishing velocity difference and a constant spatial separation between the two particles. It can be interpreted as a situation in which two particles have relaxed to the fluid motion and are then simply carried together by a uniform carrier flow with vanishing gradients. When the noise is neglected, this stable point attracts all trajectories except those located on the half line $Y = 0$ with $X < -1$. The trajectories starting in the vicinity of this half line perform very large circular loops before finally converging to the stable fixed point. Those starting exactly on the half line escape to $X = -\infty$ in a finite time and thus the separation R between the two particles vanishes in a time smaller than τ . The longitudinal velocity difference between the particles along this half-line

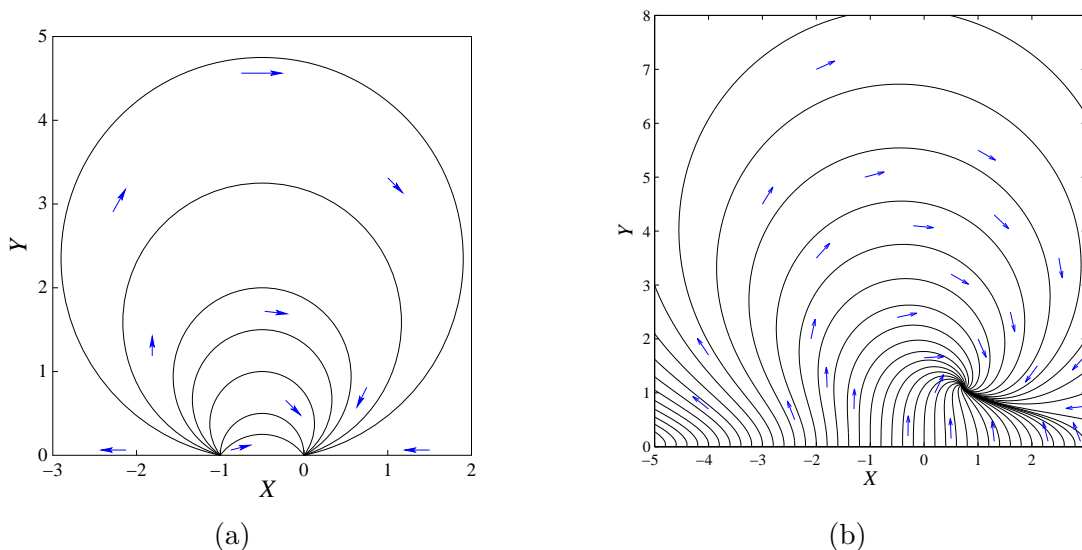


Fig. 1. Drift of the reduced system in the (X, Y) -plane for $d = 2$ (a) and $d = 3$ (b). X is the non-dimensional longitudinal velocity difference between two suspended particles; Y is the modulus of the non-dimensional velocity difference perpendicular to the particle separation.

is sufficiently large negative for the particles to cross each other within a finite time. Anyway, this happens with zero probability when noise is added. The presence of an even very small diffusion in the Y -direction prevents particles from remaining exactly on the $Y = 0$ line and thus from escaping to infinity.

In the full system, i.e. in the presence of noise, particles spend a large fraction of time in the vicinity of the stable fixed point $(0, 0)$. There, both X and Y are very small, so that the quadratic terms in the drift can be neglected. In this way the dynamics of X and Y decouple and can be well approximated by two independent Ornstein–Uhlenbeck processes. When the noise contribution is sufficiently large, the trajectory can escape this linearized regime around the stable fixed point. In particular, the noise can push the trajectory to the left of the unstable fixed point with a small value of Y . The probability of such events can be estimated from the linearized dynamics. When $St \gg 1$, the variance of the noise is very large and this probability is of order unity. In the half-plane $X < -1$, the drift acts as an accelerative term towards more negative values of X and finally dominates the diffusion. Once the (X, Y) -trajectory has reached the left of the unstable fixed point, it spends some time in the half plane $(X < -1)$ before looping back to the positive- X half plane when Y becomes sufficiently large. As we will see in subsection 4.1, such events are responsible for power-law tails with exponent -3 in the pdf of X . Moreover, these loops provide a mechanism for bringing back to the right of the stable fixed point those trajectories that went away from its left. The presence of this flux implies that $\langle X \rangle > 0$. Although such events lead to a positive Lyapunov

exponent $\lambda = \langle X \rangle / \tau > 0$, trajectories typically perform loops in the negative X 's and thus the stretching rate μ , given by the time integral of X , can be very large negative. Note that during such events, the inter-particle distance R reaches very small values which is a signature of preferential concentration.

For three dimensions, the general picture of the deterministic dynamics in the (X, Y) plane is given by Fig. 1(b). In contrast to the two-dimensional case, there is no unstable fixed point, but a unique stable fixed point that attracts all trajectories. For sufficiently large values of the Stokes number, trajectories spiral towards the stable point, which is located in the first quadrant, at $X \approx Y \approx (2St)^{1/3}$ when $St \rightarrow \infty$. Like in two dimensions, the trajectories spend a large fraction of time in its neighborhood. They thus spend more time in the half plane $(X > 0)$ than in the half plane $(X < 0)$; this clearly implies that $\lambda = \langle X \rangle / \tau > 0$. This is a signature of the fact that the motion is chaotic in three dimensions as well. Unlike in two dimensions the line $Y = 0$ acts here as a repeller. All trajectories starting there escape its vicinity with a transverse acceleration $dY/ds \propto s^{1/2}$. They reach order unity values of Y in an algebraically fast time. Despite these differences, the mechanism leading to preferential concentration is essentially the same as for $d = 2$. The trajectories which after a strong fluctuation of the noise reach the half plane $X < -1$ are accelerated to more negative values of X before looping back to the stable fixed point. Unlike in two dimensions, the probability to enter such loops cannot be estimated from the linearized dynamics in the neighborhood of the fixed point which is now far from the origin. In three dimensions, estimating this probability requires to understand how the non-linear terms affect the transition from the vicinity of the fixed point to the half plane $X < -1$.

4 Scaling behavior in the asymptotics $St \rightarrow \infty$

The behavior of the statistical quantities related to the two-particle motion is investigated in this section for the limit $St = D_1\tau \gg 1$. Following the scaling arguments developed in [29], this asymptotics is approached keeping $C = D_1/\tau^2$ constant. The limiting dynamics in two dimensions is then given by

$$\begin{aligned} d\bar{X} &= -(\bar{X}^2 - \bar{Y}^2) dt + \sqrt{2C} dB_1, \\ d\bar{Y} &= -2\bar{X}\bar{Y} dt + \sqrt{6C} dB_2, \end{aligned} \tag{21}$$

where t is the original physical time, $\bar{X} \equiv X/\tau$ and $\bar{Y} \equiv Y/\tau$. In three dimensions, the \bar{Y} drift contains an additional term of the form $4C/\bar{Y}$. The scaling arguments presented in the sequel are valid in both two and three dimensions, and are confirmed by numerical experiments.

The basic observation to derive the scaling behavior of the interesting quantities is as follows. For $St \rightarrow \infty$ and with C fixed, all statistical properties can equivalently be derived from (10)-(11) or from (21). In the former case all the statistical objects will depend only on the Stokes number, while in the latter one they only depend on the constant C . Assuming a smooth dependence on the parameters, we will derive closed differential equations which are then used to find the large St behavior.

4.1 Probability distribution function of the longitudinal velocity

The pdf $p(x; St) = \langle \delta(x - X) \rangle$ of the non-dimensional longitudinal velocity difference X is related to the pdf $\bar{p}(\bar{x}; C)$ of \bar{X} by

$$p(x; D_1 \tau) = \frac{1}{\tau} \bar{p}\left(\frac{x}{\tau}; \frac{D_1}{\tau^2}\right),$$

where the factor $1/\tau$ is due to the Jacobian of the transformation from X to \bar{X} . The equality still holds when differentiating both sides with respect to D_1 or to τ . This allows to write $\bar{p}(\bar{x}; C)$ as a solution of the following partial differential equation:

$$\bar{p} + \bar{x} \frac{\partial}{\partial \bar{x}} \bar{p} + 3C \frac{\partial}{\partial C} \bar{p} = 0,$$

which admits solutions of the form $\bar{p}(\bar{x}; C) = C^{-1/3} q(C^{-1/3} \bar{x})$. Here q is an arbitrary differentiable function. The pdf of the longitudinal velocity difference can thus be written as

$$p(x; St) \approx St^{-1/3} q(St^{-1/3} x) \quad \text{when } St \rightarrow \infty. \quad (22)$$

Hence at large Stokes numbers the non-dimensional velocity difference X typically takes values of the order of $St^{1/3}$. The same argument can be applied for estimating the order of magnitude of the approaching rate κ defined in (19). This however does not give any information on the way κ depends on the particle distance r . Equation (22) implies that the velocity difference V is proportional to $D_1 St^{-2/3}$, and thus becomes smaller when the Stokes number increases.

As shown in Fig. 2, the collapse of the pdfs of X for different values of the Stokes number confirms the scaling (22). Simulations of the reduced dynamics in two dimensions are performed by integrating explicitly the deterministic drift (see Appendix A for more details). The curve has a peak for $x > 0$ as a signature of the flux of probability from $x < 0$ to $x > 0$ induced by the loops of the (X, Y) trajectories described in the previous section.

Of particular interest is the result shown in the inset of Fig. 2, which pictures the distributions of X for several large St in log-log coordinates. The pdfs

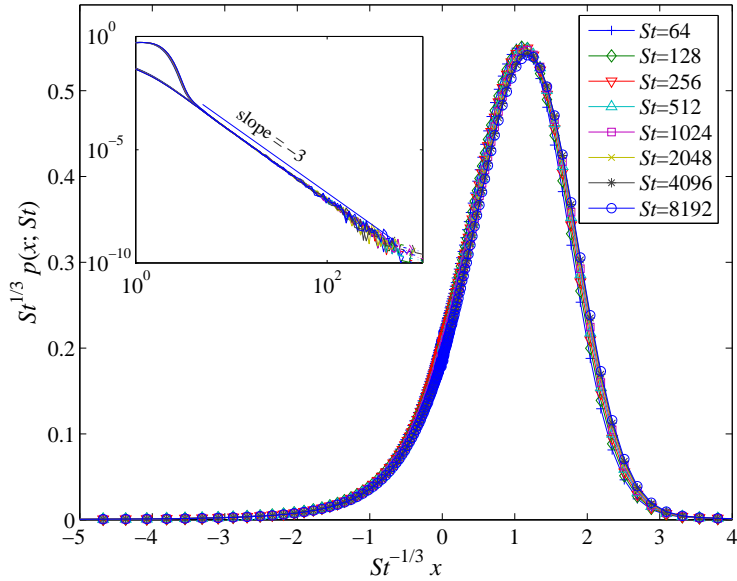


Fig. 2. Probability density function $p(x; St)$ of the non-dimensional longitudinal velocity difference X for various values of the Stokes number St in two dimensions. Inset: same in log-log coordinates.

of the velocity difference display power-law tails with exponent -3 over two decades for both positive and negative values of X . This is again a signature of the very large loops characteristic of the dynamics in the (X, Y) plane. The observed power-law tails can be heuristically explained for large values of St by considering the limiting dynamics (21). The loops reaching large negative values of X are then approximated by circles passing by $(0, 0)$. In order to explain the algebraic tails in the pdf of the longitudinal velocity difference, we make a very crude approximation of the dynamics. When the trajectories are within a distance order unity of $(0, 0)$, the noise dominates and \bar{X} and \bar{Y} behave as two independent Brownian motion. At distances from the origin which are larger than unity, the drift dominates and the trajectories are circles. Figure 3 sketches this simplification of the dynamics. We now turn to estimate the cumulative distribution function $P^<(x) = \text{Prob}(\bar{X}(s) < x)$ for $x \ll -1$. The above simplification of the dynamics leads to considering two separate contributions to $P^<$: (i) the probability to start a large loop that goes to the left-hand side of x and (ii) the fraction of time spent at $X < x$, once such a loop is initiated.

We first estimate contribution (i). To start a large loop that reaches values of \bar{X} smaller than x , the trajectory must be at $\bar{X} \approx -1$ with \bar{Y} sufficiently small. More precisely, the trajectory must be below the circle touching $\bar{X} = x$ when exiting the region where the noise dominates. This circle, which is represented by dots in Fig. 3, is defined by $\bar{X}^2 + (\bar{Y} + x)^2 = x^2$; for $\bar{X} = -1$ and x large, one has $\bar{Y} \propto (-x)^{-1}$. The probability to start a large loop is thus given by the

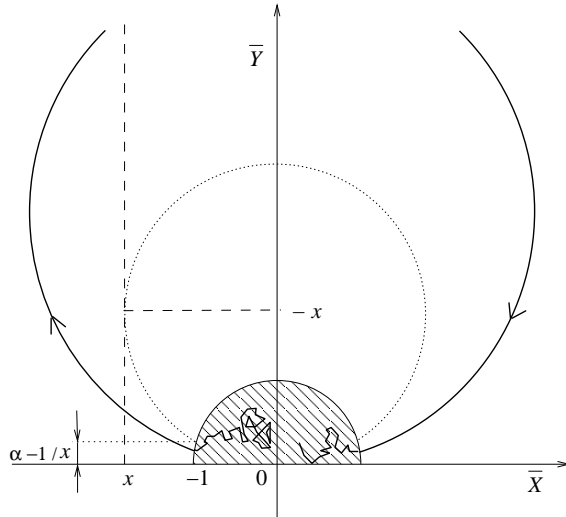


Fig. 3. Sketch of the simplified dynamics in the (\bar{X}, \bar{Y}) plane. A typical trajectory performing a large loop is represented as a bold line. At distances less than unity from the origin (striped area), the noise dominates and the trajectory is approximated by a pure Brownian motion. At larger distances, the drift dominates and the trajectories perform circular loops. In order to reach values of \bar{X} smaller than $x \ll -1$, the trajectory must exit the striped area with $\bar{Y} = o(1/|x|)$.

probability that the two-dimensional Brownian motion (starting, for instance, at the origin) exits the circle of radius 1 from the infinitesimal interval $\bar{X} = -1$ and $0 \leq \bar{Y} \leq (-x)^{-1}$. This probability is clearly $\propto (-x)^{-1}$.

We next estimate the contribution (ii) coming from the fraction of time spent at $\bar{X} < x$ on a sufficiently large loop. It is easily checked from (21) that when neglecting noise and rescaling time by a factor $\propto R^{-1}$ the circular trajectories of radius R become circles with radius of order unity. This implies that the trajectories spend a time of order $(-x)^{-1}$ in the half plane $\bar{X} < x$, whence a second contribution also $\propto (-x)^{-1}$.

Lumped together, the two contributions (i) and (ii) imply that $P^<(x) \propto (-x)^{-2}$. Hence the pdf of the longitudinal velocity difference has a power-law tail with exponent -3 at large negative values. During the large loops, the trajectories in the (\bar{X}, \bar{Y}) plane also reach large positive values of \bar{X} and of \bar{Y} and this gives again a fraction of time $\propto x^{-1}$ spent at both $\bar{X} > x \gg 1$ and $\bar{Y} > x \gg 1$. We hence have the same algebraic tail with exponent -3 for the pdf of both the longitudinal and the transversal velocity difference at large positive values.

This argument cannot be straightforwardly applied to the three-dimensional case. As stated in the previous section the probability for the trajectories to enter a large loop cannot be directly estimated by linearizing the dynamics in the vicinity of the fixed point. Moreover, the numerical simulations can hardly

be extended to the reduced system in three dimensions. They cannot be based on an explicit integration of the drift and are generally unstable. At present, we do not know whether or not the power-law behavior $\propto |x|^{-3}$ for the pdf of X also holds in three dimensions.

4.2 The Lyapunov exponent and the stretching rate

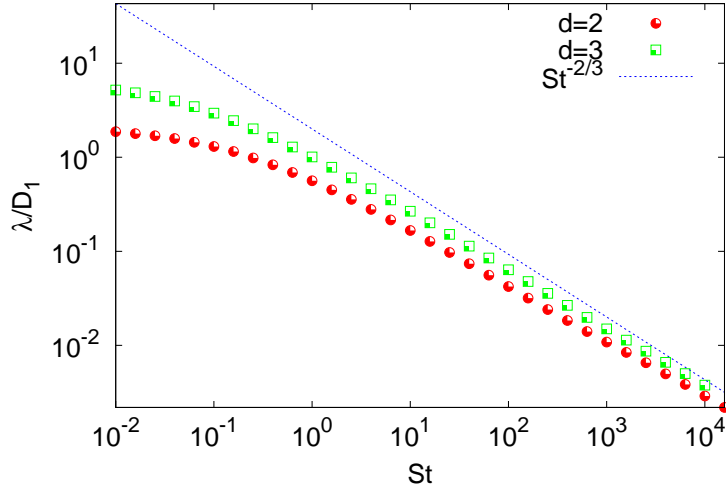


Fig. 4. Lyapunov exponent λ as a function of the Stokes number St in log-log coordinates in both two and three dimensions.

A direct consequence of (22) is that the Lyapunov exponent given by $\langle X \rangle / \tau$ behaves as

$$\lambda \approx \alpha C^{1/3} = \alpha D_1 St^{-2/3}, \quad (23)$$

where $\alpha = \int dz z q(z)$ is a constant. This result was obtained in [29] where it is shown that it holds even for compressible flows. Figure 4 confirms numerically the power-law behavior (23) in both two and three dimensions. Note that the asymptotic regime is reached only for rather large values of St (typically larger than 100).

We now extend the scaling arguments of [29] to the rate function H of the large deviations of the stretching rate μ defined in (14). As for X , the asymptotic form for the pdf of μ given in (15) is equated with the pdf obtained from the system depending only on C . After differentiating with respect to D_1 and τ , we obtain that $H(\rho = \tau\mu; St)$ obeys the following partial differential equation:

$$\rho \frac{\partial}{\partial \rho} H + 3 St \frac{\partial}{\partial St} H = H.$$

From this relation the scaling form

$$H(\mu\tau; St) \approx St^{1/3} h(St^{-1/3}\mu\tau) \quad (24)$$

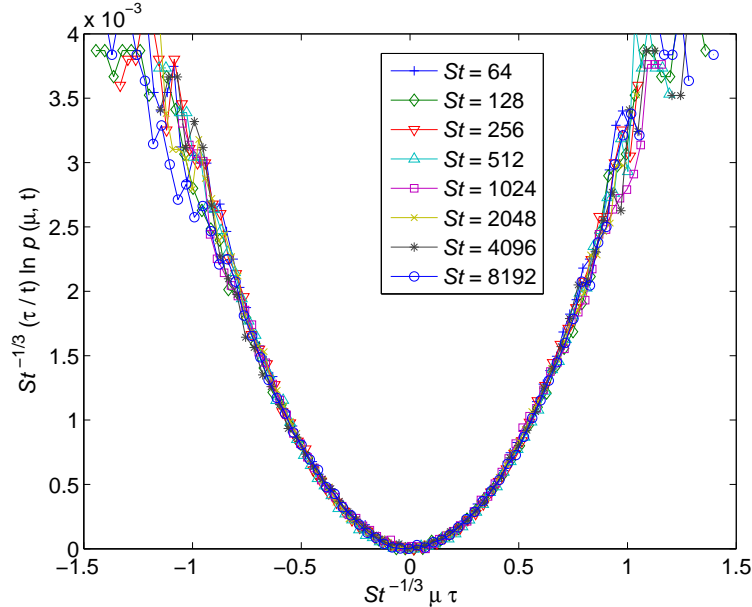


Fig. 5. Rate function of the finite-time Lyapunov exponent μ .

can be derived. This asymptotic behavior for the rate function of the large deviations of the stretching rate is confirmed by two-dimensional numerical experiments (see Fig. 5).

We have seen in the previous subsection that the Lyapunov exponent tends to zero as $St^{-2/3}$ in the limit $St \rightarrow \infty$. From the $St^{1/3}$ prefactor in the asymptotic form (24) and assuming, for instance, that H is a quadratic function, it is easily checked that the typical fluctuations of the stretching rate are $O(St^{-5/6})$. This indicates the tendency of the stretching rate to become more and more sharply distributed around the Lyapunov exponent when $St \gg 1$. As expected, the dynamics indeed tends to be less and less intermittent in this limit.

5 Saturation of the correlation dimension

This section addresses the statistical characterization of clustering mostly in terms of the correlation dimension of the particle spatial distribution introduced in Section 3.2. This quantity controls the behavior of the probability that two particles are separated by a small distance. We also comment on the large Stokes number behavior of the approaching rate. This quantity provides a statistical measure of the rate of collisions between particles.

Particles with infinite inertia ($St = \infty$) need an infinite time for their velocity to relax to that of the fluid flow. In other terms they have a ballistic dynamics: they move freely maintaining their initial velocity. Such particles hence dis-

tribute uniformly in phase space and the correlation dimension of their spatial distribution equals the space dimension, i.e. $\mathcal{D}_2 = d$. Furthermore, as the velocities of the particles become uncorrelated, the exponent γ characterizing the small-scale behavior of the approaching rate (see (20)) is expected to coincide in this asymptotics with the correlation dimension. Thus, for $St \gg 1$ one has $\mathcal{D}_2 \simeq \gamma \simeq d$.

Following the strategy devised in the previous section, we now try to determine the corrections to this limiting behavior at large but finite values of St with the help of scaling arguments. For this purpose, we make use of relation (18) between the correlation dimension \mathcal{D}_2 and the rate function H of the large deviations of the stretching rate μ . Assuming the large Stokes number asymptotic form (24) for the latter, equation (18) can be written as

$$\min_{\rho} \left[\mathcal{D}_2 \rho + St^{1/3} H \left(St^{-1/3} \rho \right) \right] = 0.$$

Introducing $\alpha = St^{-1/3} \rho$, this leads to the following relation

$$\min_{\alpha} [\mathcal{D}_2 \alpha + H(\alpha)] = 0,$$

which does not involve the Stokes number. For consistency with the limit $St \rightarrow \infty$ we have $\mathcal{D}_2(St) = d$. The scaling approach thus fails to catch any deviation from a uniform distribution. This suggests two possibilities. The first one is that the deviations from the limiting value can only be caught by subleading terms in the asymptotic form of H . The second possibility is that \mathcal{D}_2 saturates to d for Stokes numbers larger than a critical value St^\dagger . Even if we do not have a rigorous proof to decide between these two possibilities, we present in the following strong evidences in favor of the latter scenario.

The saturation of the fractal correlation dimension to the space dimension can be understood by considering the particle motion in the full position-velocity phase space. As stated in the Introduction, the inertial particle dynamics is dissipative in phase space and the particle trajectories converge to a random attractor. This dynamically evolving set is typically characterized by a multifractal measure with a spectrum of dimensions $\overline{\mathcal{D}}_q$ [36,37,19]. In particular, the correlation dimension $\overline{\mathcal{D}}_2$ in phase space is the straightforward generalization of \mathcal{D}_2 . It can be defined through the small-scale algebraic behavior of the probability $\overline{P}_2(r)$ to find two particles at a distance less than r in phase space:

$$\overline{P}_2(r) \sim r^{\overline{\mathcal{D}}_2} \quad \text{for} \quad r \rightarrow 0.$$

To evaluate a distance in phase space we make use of the Euclidean norm $\sqrt{|\mathbf{R}|^2 + |\mathbf{V}/D_1|^2}$, where we choose to divide \mathbf{V} by the typical gradient D_1 of the fluid flow in order to obtain a quantity with dimension of a length-scale. Clearly, the particle positions are obtained by projecting the particle distance

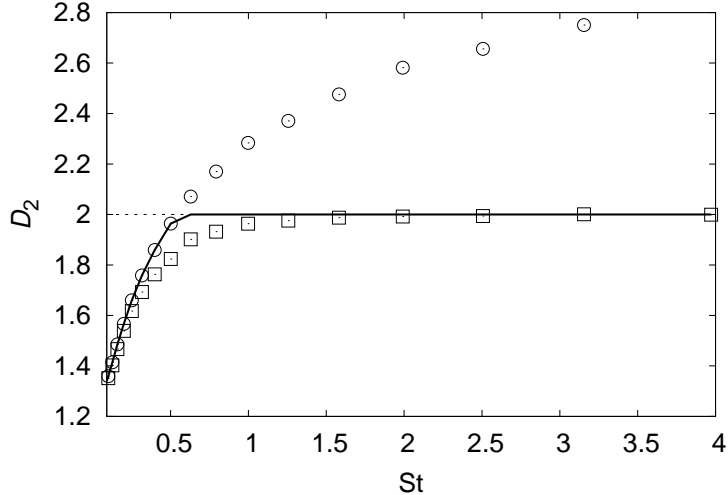


Fig. 6. Correlation dimension in physical space \mathcal{D}_2 (empty squares) and in phase space $\overline{\mathcal{D}}_2$ (empty circles) as a function of St . The solid curve represents the prediction based on the projection formula (25). The exponents were obtained by averaging the local slopes (logarithmic derivatives) of the pair separation probability. See text and Fig. 7 for a discussion on the behavior of the local slopes.

from the $(2 \times d)$ -dimensional phase space onto the d -dimensional physical space. It is then tempting to apply rigorous results that have been obtained on the projection of fractal sets [39,40]. In particular, it can be shown that for *almost all* projections, the correlation dimension of the projection of a random fractal set is the minimum of the correlation dimension of the object in the full space and of the dimension of the subspace onto which it is projected. In our case, this would lead to

$$\mathcal{D}_2 = \min\{d, \overline{\mathcal{D}}_2\}. \quad (25)$$

In the limit of large Stokes numbers, the particle motion becomes ballistic and thus conservative, meaning that the trajectories fill the whole phase space and $\overline{\mathcal{D}}_2 \rightarrow 2d$. This, together with the projection formula (25), suggests that there exists a critical value St^\dagger of the Stokes number such that $\mathcal{D}_2(St) = d$ for all $St \geq St^\dagger$. However, determining whether \mathcal{D}_2 saturates above St^\dagger or whether it approaches d asymptotically, depends on the genericity of the projection from phase space onto the physical space. Unfortunately, there is *a priori* no reason for assuming some kind of isotropy in phase space which would justify the validity of (25).

We are therefore led to investigating this issue numerically. Following [25], we estimate both the correlation dimensions \mathcal{D}_2 and $\overline{\mathcal{D}}_2$ by means of time averages performed following a particle pair during a very long time T (here typically $T = 10^8 - 10^9$). We then evaluate the probability to find the two particles at a distance $\leq r$ (using both the phase-space and real-space norms). The use of Lagrangian averages is justified by invoking ergodic properties of the

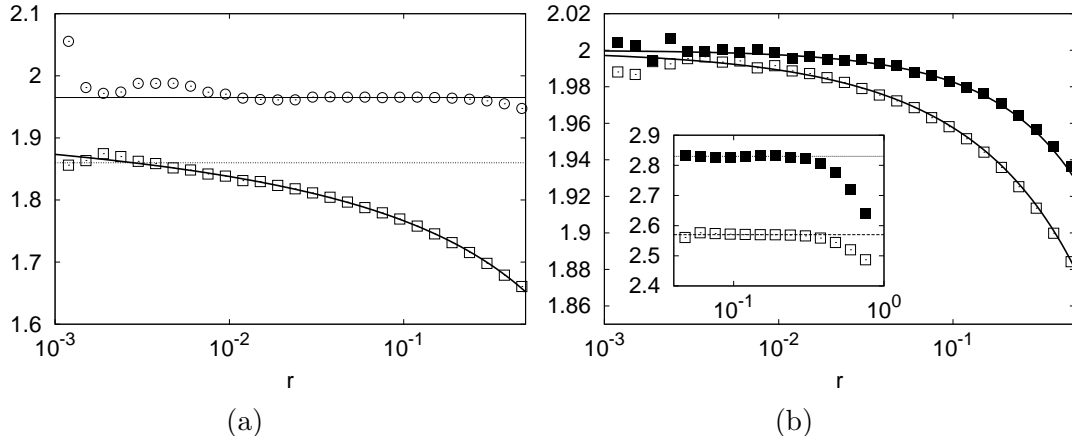


Fig. 7. (a) Logarithmic derivative $(d \log P_2(r))/(d \log r)$ of the pair distance probability in real space (empty boxes) and in phase space (empty circles) for $St = 0.5$. The solid straight line is at the estimated $\overline{\mathcal{D}}_2 = 1.965$, the dotted straight line is at the value 1.86 obtained by averaging the correlation dimension in real space in the range $[10^{-3} : 10^{-2}]$. The thick black line corresponds to a fit of the local slopes by assuming a superposition of two power laws, i.e. assuming $P_2(r) = Ar^a + Br^2$ (see text for a discussion). (b) Logarithmic derivative $(d \log P_2(r))/(d \log r)$ vs r for $St = 2.0$ (empty boxes) and $St = 4$ (full boxes). The curves are obtained by using (26) as a fitting function. The inset displays $(d \log \overline{P}_2(r))/(d \log r)$ vs r for $St = 2.0$ (empty boxes) and $St = 4$ (full boxes), for which $\overline{\mathcal{D}}_2 \approx 2.58$ and 2.83 respectively.

particle trajectories (see [25] for a detailed discussion). To have a statistically steady distribution, we assume periodic boundary conditions on the square $[0 : 1] \times [0 : 1]$. This may lead to anisotropies at distances $O(1)$ which however disappear at the small scales we are interested in. Details of the simulation method are discussed in Appendix B.

We first scan a broad range of Stokes numbers to measure the probabilities $P_2(r)$ and $\overline{P}_2(r)$ in physical and in phase space, respectively. We then average the local slopes obtained from the logarithmic derivative $(d \ln P_2(r))/(d \ln r)$ to obtain an estimate of the two correlation dimensions. Our numerical findings are summarized in Fig. 6 in which \mathcal{D}_2 and $\overline{\mathcal{D}}_2$ are represented as a function of St . These results seem to be in contradiction with the projection formula (25); thus projecting onto the physical space may actually be atypical. It is particularly worth noticing that even when $\overline{\mathcal{D}}_2 < d$ we find $\mathcal{D}_2 < \overline{\mathcal{D}}_2$. Note that the same kind of observation has been made in *ad hoc* examples where the projection is trivially typical, such as random fractal sets in three dimensions projected on randomly oriented planes (see, e.g., [41]). This suggests to reconsider with more care the analysis of the data by performing a closer inspection of the local slopes (see Fig. 7a and b). As one can see, the naive estimation in terms of averages of the local slopes, although appropriate for measuring $\overline{\mathcal{D}}_2$ in phase space,² might not be justified for \mathcal{D}_2 . As exemplified in Fig. 7a and

² In this case, there always exists a range of scales where the logarithmic derivative

7b, the local slopes $(d \ln P_2(r))/(d \ln r)$ are curved, indicating a behavior that differs from a pure power law. This observation is made both below and above the potential critical Stokes number $St^\dagger \approx 0.6$ for which $\overline{\mathcal{D}}_2(St^\dagger) = d = 2$.

Similarly to what has been observed in other systems exhibiting multifractal behavior [42], one can be tempted to interpret the curvature of the local slopes by the presence of sub-dominant terms leading to the superposition of two power laws. Indeed, as sufficiently small scales require an amount of statistics that can hardly be reached numerically, subleading terms typically contaminate the scaling behavior. We hence make the *Ansatz* that the probability distribution of the two-particle separation r can be approximated by $P_2(r) \simeq Ar^a + Br^b$ at the spatial scales we resolve. In our case it is rather clear how to guess the exponents a and b for $St < St^\dagger$. Since $\overline{\mathcal{D}}_2 < d$ in this range of Stokes numbers, one expects from (25) the projected set to have dimension $\mathcal{D}_2 = \overline{\mathcal{D}}_2$. However, at such values of St there is a contribution coming from caustics [43,25]. With a non-zero probability, particles can come sufficiently close to each other with quite different velocities. Once projected onto the physical space, these caustics will appear as spots of uncorrelated particles, and hence, locally, the correlation dimension will be $\mathcal{D}_2 = d = 2$. This (indeed very) crude argument suggests that

$$P_2(r) = Ar^{\overline{\mathcal{D}}_2} + Br^2. \quad (26)$$

As shown in Fig. 7, this fitting form is actually in very good agreement with the behavior of the local slopes. Indeed the validity of (26) was confirmed by several experiments which consisted in varying the number of free parameters in the fit (i.e. by fixing or not the values of the exponents a and b). It is interesting to note that also for $St > St^\dagger$ the asymptotic form (26) approximates very well the data, even though the simple argument we sketched is not applicable for such values of the Stokes number. Thus, to summarize, we found that for values of St near St^\dagger , the probability $P_2(r)$ is well approximated at small scales by the superposition of two power laws with exponents $\overline{\mathcal{D}}_2$ and the dimension of the physical space d . The first power-law gives the leading behavior for $St < St^\dagger$ and is related to the fractal nature of the particle distribution in the position-velocity phase space. The second power-law gives the behavior for $St > St^\dagger$ and is related to the presence of caustics in the particle dynamics. This picture gives strong evidence in favor for the saturation to the space dimension d of the correlation dimension \mathcal{D}_2 for sufficiently large values of the Stokes number.

We now make a brief comment on the implication of saturation for the behavior of the approaching rate. Clearly, in the limit $St \rightarrow \infty$, particles, move ballistically and hence can approach each other within an arbitrary small distance with order unity velocity differences. One thus expects the exponent

is fairly constant.

γ of the approaching rate defined in (20) to tend to d . As in the case of the correlation dimension \mathcal{D}_2 the deviations from this limiting value cannot be determined by scaling arguments. The possible saturation of \mathcal{D}_2 however affects γ . Indeed this saturation can be interpreted in terms of a dominant contribution of caustics that could imply the saturation of γ to d for sufficiently large Stokes numbers. As shown in the next section, though numerical experiments confirm this scenario, saturation cannot be studied with as much detail as for \mathcal{D}_2 . In particular, there is at the moment no simple phenomenological argument able to guess the form of the subleading terms, and to understand if saturation for γ takes place at St^\dagger or at a different value.

6 The case of finite Stokes numbers

Apart from its validity for the large Stokes asymptotics, the study of inertial particles suspended in δ -correlated Gaussian flows is interesting *per se*, even for $St < St^\dagger$. Indeed, as found for Lagrangian and scalar transport of tracers [33], this model catches behaviors similar to those characteristic of more realistic suspensions, that is of time-correlated [25] or turbulent [1,44] flows. Though much simpler, this model entails difficulties when tackled with purely analytical tools and for arbitrary Stokes numbers. We shall therefore stick mostly to a numerical analysis. In particular, the correlation dimension and its dependence on the Stokes number is studied when St is not very large.

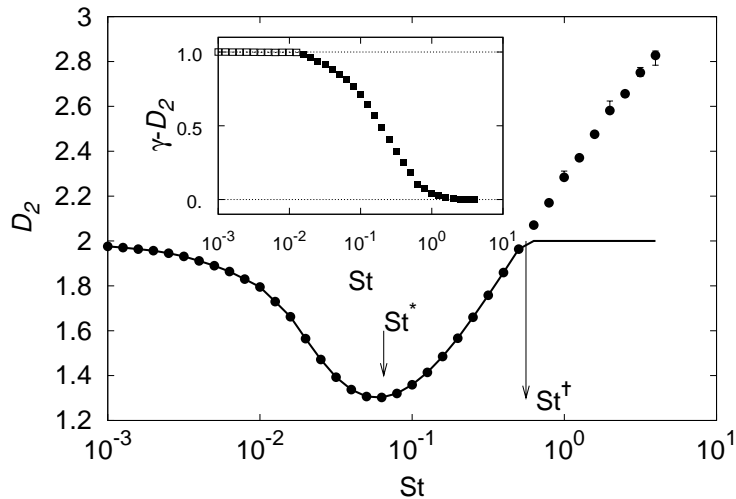


Fig. 8. Scaling exponents as a function of St . Data refer to: the correlation dimension in real space \mathcal{D}_2 (thick solid line), which has been corrected for St close and larger than St^\dagger using (25) and the correlation dimension in phase space \mathcal{D}_2 (full circles). Inset: $\gamma - \mathcal{D}_2$ vs St . Note the plateaus at 1 at small St and at 0 for large St .

The main numerical findings are summarized in Fig. 8: the correlation dimensions \mathcal{D}_2 and $\overline{\mathcal{D}}_2$ in physical space and in phase space, respectively, as well

as the exponent γ , characterizing the approaching rate, are represented as a function of the Stokes number.

The main feature is that for $St = St^* \approx 0.07$, the correlation dimension has a minimum corresponding to a maximum of clustering. The presence of such an “optimal” Stokes number St^* for the formation of particle clusters (here quantified by \mathcal{D}_2) is a generic feature that has also been observed using other indicators, such as the deviation of the particle number density from a uniform distribution [1,15] or the Lyapunov dimension [45]. In turbulent flows, this Stokes number was found to be of order unity, that is the particle response time is of the order of the Kolmogorov eddy turnover time. According to the standard phenomenological picture (see, e.g., [1]), this can be interpreted in terms of an optimal response time for the particles that anti-correlate with the vortical structures of the flow. This is responsible for the accumulation of particles in strain regions and, hence, for the formation of inhomogeneities in their spatial distribution. This appealing picture based on the presence of persistent structures in the fluid flow can, of course, not be applied to white-in-time random flows. Here, the mechanisms responsible for an optimal response time of the particles seem to have a purely dynamical origin. In our settings the only relevant time scale is $1/D_1$ which is a Lagrangian time scale (essentially the inverse of the Lyapunov exponent of fluid tracers). Even if we cannot exclude that time-correlated and time-uncorrelated flows are governed by different mechanisms, our conjecture is that particle clustering has a purely Lagrangian origin. A deeper heuristic understanding of such mechanisms is still lacking.

It is of interest to observe that at small Stokes numbers $St \ll St^*$, the behavior in uncorrelated carrier flows differs markedly from what is observed in correlated flows. Indeed, as seen from Fig. 9, the dimension deficit $2 - \mathcal{D}_2$ is proportional to St . This is in clear contrast with the $\propto St^2$ behavior found and predicted in both random time-correlated [24,19] and turbulent [22,21] flows. The scaling behavior we observe at small Stokes numbers is rather clean (see inset of Fig. 9). For $St \ll St^\dagger$, the subleading terms discussed in the previous section can hardly be detected and $\mathcal{D}_2 \approx \overline{\mathcal{D}}_2 \approx \gamma - 1$. This behavior is shown in the insets of Figs. 8 and 9. These measurements suggest that in this regime the particle velocities are defining a smooth velocity field. As particles do not distribute homogeneously in space, one expects this field to be compressible. This leads us to conjecturing that the small Stokes number asymptotics can eventually be approximated with an expansion of the particle velocity as a function of the flow velocity. The validity of this expansion has been shown for correlated flows where it has been successfully used [46,20]. However this approach cannot be straightforwardly applied to the δ -correlated case where the time scale of the fluid is the fastest of the system. Tackling this asymptotics requires the use of standard techniques of singular perturbation theories [47] (see also [48]), which is beyond the scope of the present work.

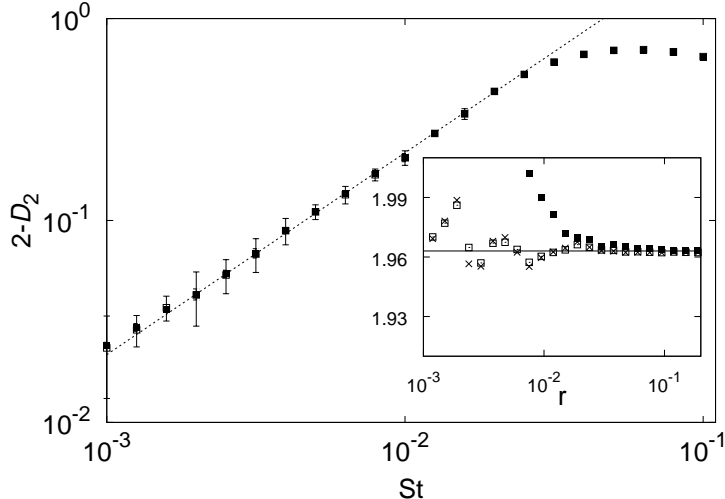


Fig. 9. Dimension deficits $2 - \mathcal{D}_2$ (empty boxes) and $2 - \overline{\mathcal{D}}_2$ (full boxes) as a function of St in log-log coordinates. Note the remarkable overlap that almost hides the empty boxes. The dashed straight line is the result of a linear fit $2 - \mathcal{D}_2 = 21.6St$. Inset: Logarithmic derivatives $(d \log P_2(r))/(d \log r)$ (empty boxes), $(d \log \overline{P}_2(r))/(d \log r)$ (full boxes), and $[(d \log \kappa_2(r))/(d \log r) - 1]$ (crosses) for $St = 1.6 \cdot 10^{-3}$, illustrating the typical quality of the scaling for $St \ll 1$.

The exponents characterizing the scaling of the approaching rate, as shown in the inset of Fig. 8, deviate from the small St asymptotics $\gamma = \mathcal{D}_2 + 1$ already for $St < St^*$. They actually approach rapidly the large St asymptotics $\gamma \simeq \mathcal{D}_2$. This means that velocity differences of close particles become less and less correlated, i.e. $|\mathbf{V}| \sim |\mathbf{R}|^0$. Caustics seem to dominate the two-particle statistics already at intermediate values of the Stokes number.

We finally mention that we have performed similar numerical experiments in three dimensions. Although they involve fewer statistics, they reproduce qualitatively the same general picture. This indicates that, in spite of its simplicity, studying the case of δ -correlated flows may give insight into general mechanisms that are at play in more realistic flows.

7 Concluding remarks

In this paper it was shown that the fluid flow along particles with large inertia can be modeled by a Gaussian, δ -correlated in time random process. We exploited this to quantify the statistical properties of two particle motions in the large Stokes number asymptotics. The dynamics of particle separation in position-velocity phase space can be reduced to three stochastic differential equations involving the distance, and the longitudinal and transverse velocity differences. Focusing mostly on two dimensions, we reinterpreted within

this approach many aspects of inertial particle dynamics such as, for instance, preferential concentration.

We made use of scaling arguments to determine the asymptotic behavior of the Lyapunov exponent, of the distribution of the stretching rate and of the velocity differences, predictions which are confirmed numerically. The results are expected to hold in generic flow and should apply in realistic situations which involve particles with sufficiently large inertia. It is therefore tempting to check the validity of the scaling arguments by investigating the large Stokes number behavior in turbulent carrier flows. Concerning the small-scale behavior of the spatial distribution of particles, we presented strong evidences that the correlation dimension saturates to the spatial dimension when the Stokes number exceeds a threshold value St^\dagger . To detect numerically this saturation, it was necessary to control the subleading contribution to the pair separation distribution function. We extended our study to values of the Stokes number where the model loses its physical relevance. For $St < St^\dagger$, we showed that particles transported by a δ -correlated flow reproduce the main qualitative features of particle clustering observed in real settings. Even though the small St asymptotics seems to be restricted to time uncorrelated situations, an “optimal” Stokes number St^* for particle clustering is observed as is the case in turbulent flows. Its existence in structure-less δ -correlated flows questions the classical phenomenological explanation.

Our investigation of the probability distribution of the velocity difference between two particles revealed the presence of power-law tails with exponent -3 for $St \gg 1$. We presented a phenomenological argument relating this algebraic behavior with those events where the particles approach each other ballistically. It is worth noticing that the presence of power-law tails leads to the divergence of the high-order moments of the velocity difference. This can be one of the reasons why, so far, it was not possible to provide analytical solutions of the Fokker-Planck equations associated to the stochastic model. It is interesting to mention other difficulties that have been encountered elsewhere in the analytical treatment of this model, such as the non-analyticity of the Lyapunov exponent for $St \rightarrow 0$ (see, e.g., [29] and references therein).

We conclude by stressing that a phenomenological understanding of the relative motion of inertial particles in turbulent flows may benefit from approaching the problem in terms of the reduced variables discussed here. In particular, it would be very informative to study the probability distribution of the components of the velocity difference, not only to check whether or not the -3 tails are present but also to understand its behavior at finite Stokes numbers.

Acknowledgements

We are grateful to L. Biferale, A. Celani, G. Falkovich, A. Fouxon, U. Frisch, P. Horvai and S. Musacchio for useful discussions and remarks. Partial support by the EU under the research training network HPRN-CT-2002-00300 “Stirring and Mixing” is acknowledged. The stay of R.H. in Nice was supported by the Zeiss-Stiftung. M.C. acknowledges the Max Planck Institute for the Physics of Complex Systems for computational resources.

Appendix

Numerical Methods

On the numerical side we developed both a fast and efficient code for the direct integration of (6), and for the stochastic equations of the reduced model (10)-(11).

A Integration of the reduced model

For the direct integration of the reduced model (10)-(11) in two dimensions we used a straightforward Euler–Ito scheme. The deterministic part of the evolution was explicitly integrated in order to avoid particles from escaping to infinity. Indeed far from the stable and unstable fixed points (see Fig. 1(a)) the deterministic drift becomes very large and affects the numerical precision. The explicit solver for the deterministic part of the dynamics is easily obtained in two dimensions by noticing that equations (10) and (11) for X and Y can be written as

$$\frac{dZ}{dt} = -Z - Z^2,$$

where $Z = X + iY$. This equation can be directly integrated as [26]

$$Z(t + \Delta t) = \frac{Z(t) \exp(-\Delta t)}{1 + Z(t)(1 - \exp(-\Delta t))}.$$

Then the noise term is added in the usual way by using the Euler-Ito scheme. This integration method is very efficient and has been used to evaluate the large deviations of the finite-time Lyapunov exponent and of the Lyapunov exponent itself.

In three dimensions, due to the $1/Y$ term the model equations are very stiff and it is rather difficult to develop a stable and efficient integration scheme. We thus used the Lagrangian method described below.

B Lagrangian integration of two-particle dynamics

The two-point motion (6) can be numerically integrated in a very efficient way by following [49]. In practice one simply needs to generate the random relative velocities according to a white-noise Gaussian process with a correlation function given by (4)-(5). This can be done easily because the correlation matrix d_{ij} in (5) is symmetric and positive definite. The latter property allows us to use the Cholesky decomposition of the correlation matrix,

$$d_{ij}(r) = L_{ik}L_{jk}.$$

L_{ij} being a non singular lower triangular matrix. The integration of (6) can thus be performed with a standard Euler-Ito scheme

$$\begin{aligned} R_i(t + \Delta t) &= R_i(t) + \Delta t V_i(t), \\ V_i(t + \Delta t) &= \left(1 - \frac{\Delta t}{\tau}\right) V_i + \frac{1}{\tau} \sqrt{2\Delta t} L_{ij} \eta_j, \end{aligned}$$

where $i, j = 1 \dots d$, Δt is the discretized time step and the η_j 's are d independent white noises.

The numerical procedure is thus as follows. Given the separation \mathbf{R} between two particles, the correlation matrix $d_{ij}(r = |\mathbf{R}|)$ is computed from (5), and L_{ij} is obtained by means of an efficient algorithm (see, e.g., [50]). The d independent Gaussian variables η_j are generated and the velocity is obtained as $L_{ij}\eta_j$. In two spatial dimensions the latter procedure is particularly efficient. Indeed, the velocity differences associated to the particle separation $\mathbf{R} = (x, y)$ can be simply written as:

$$\begin{aligned} \delta u_x(t) &= \sqrt{D_1}(x\eta_1 - y\eta_2) \\ \delta u_y(t) &= \sqrt{D_1}(y\eta_1 + x\eta_2). \end{aligned}$$

The evolution of the separation (6) is supplemented by periodic boundary conditions. This is required for studying the stationary spatial distribution of particles. These boundary conditions do not affect the small scales properties we are interested in.

This procedure has the advantage of working in a quasi-Lagrangian frame, i.e.

directly with the particle relative position and the velocity difference. Furthermore, it can be easily generalized to rough flows. We used it for computing the pair-separation probability distribution, the phase-space correlation dimension and the approaching rate (see Section 6). The algorithm we set up is fast enough to allow us to reach statistics up to times of orders $10^8 - 10^9$ (which for the smaller values of the Stokes number corresponds to $10^{13} - 10^{14}$ time steps) in a few hours on a PC.

References

- [1] J.K. Eaton and J.R. Fessler, “Preferential concentrations of particles by turbulence,” *Int. J. Multiphase Flow* **20**, 169 (1994).
- [2] M. Pinsky and A. Khain, “Turbulence effects on droplet growth and size distribution in clouds—a review,” *J. Aerosol Science* **28**, 1177 (1997).
- [3] G. Falkovich, A. Fouxon, and M.G. Stepanov, “Acceleration of rain initiation by cloud turbulence,” *Nature* **419**, 151 (2002).
- [4] R.A. Shaw, “Particle-turbulence interactions in atmospheric clouds,” *Ann. Rev. of Fluid Mech.* **35**, 183 (2003).
- [5] B.J. Rothschild and T.R. Osborn, “Small-scale turbulence and plankton contact rates,” *J. Plankton Res.* **10**, 465 (1988).
- [6] D. Lewis and T. Pedley, “Planktonic contact rates in homogeneous isotropic turbulence: Theoretical predictions and kinematic simulations,” *J. Theor. Biol.* **205**, 377 (2000).
- [7] I. dePater and J. Lissauer, *Planetary Science* (Cambridge University Press, Cambridge 2001).
- [8] S. Weidenschilling, “Aerodynamics of solid bodies in the solar nebula,” *Mont. Not. R. Astr. Soc.* **180**, 57 (1977).
- [9] S. Post and J. Abraham, “Modeling the outcome of drop-drop collisions in Diesel sprays,” *Int. J. Multiphase Flow* **28**, 997 (2002).
- [10] T. Elperin, N. Kleorin, M.A. Liberman, V.S. L’vov, A. Pomyalov, and I. Rogachevskii, “Clustering of fuel droplets and quality of spray in diesel engines,” preprint nlin.CD/0305017.
- [11] P. Villedieu and J. Hylkema, “Modèles numériques lagrangiens pour la phase dispersée dans les propulseurs à poudre,” Technical Report ONERA (March 2000).
- [12] M.R. Maxey and J. Riley, “Equation of motion of a small rigid sphere in a nonuniform flow,” *Phys. Fluids* **26**, 883 (1983).

- [13] J.R. Fessler, J.D. Kulick, and J.K. Eaton “Preferential concentration of heavy particles in a turbulent channel flow,” *Phys. Fluids* **6**, 3742 (1994).
- [14] W.C. Reade and L.R. Collins, “Effect of preferential concentration on turbulent collision rates,” *Phys. Fluids* **12**, 2530 (2000).
- [15] K.D. Squires and J.K. Eaton. “Preferential concentration of particles by turbulence,” *Phys. Fluids A* **3**, 1169 (1991).
- [16] J. Bec, L. Biferale, G. Boffetta, A. Celani, M. Cencini, A. Lanotte, S. Musacchio, and F. Toschi “Acceleration statistics of heavy particles in turbulence,” to appear in: *J. Fluid Mech.*, preprint: nlin.CD/0508012.
- [17] J.-P. Eckmann and D. Ruelle, “Ergodic theory of chaos and strange attractors,” *Rev. Mod. Phys.* **57**, 617 (1985).
- [18] L. Arnold, *Random Dynamical Systems* (Springer Monographs in Mathematics, Berlin/New York 2003)
- [19] J. Bec, “Multifractal concentrations of inertial particles in smooth random flows,” *J. Fluid Mech.* **528**, 255 (2005).
- [20] E. Balkovsky, G. Falkovich, and A. Fouxon, “Intermittent distribution of inertial particles in turbulent flows,” *Phys. Rev. Lett.* **86**, 2790 (2001).
- [21] J. Chun, D.L. Koch, S.L. Rani Aruj Ahluwala, L.R. Collins, “Clustering of aerosol particles in isotropic turbulence,” *J. Fluid Mech.* **536**, 219 (2005).
- [22] G. Falkovich and A. Pumir, “Intermittent distribution of heavy particles in a turbulent flow,” *Phys. Fluids* **16**, L47 (2004).
- [23] H. Sigurgeirsson and A.M. Stuart, “A model for preferential concentration,” *Phys. Fluids* **14**, 4352 (2002).
- [24] L.I. Zaichik and V. Alipchenkov, “Pair dispersion and preferential concentration of particles in isotropic turbulence,” *Phys. Fluids* **15**, 1776 (2003).
- [25] J. Bec, A. Celani, M. Cencini, and S. Musacchio, “Clustering and collisions of heavy particle in random smooth flows,” *Phys. Fluids* **17** 073301 (2005).
- [26] L.I. Piterbarg, “The top Lyapunov exponent for stochastic flow modeling the upper ocean turbulence,” *SIAM J. Appl. Math.* **62**, 777 (2002)
- [27] B. Mehlig and M. Wilkinson, “Coagulation by random velocity fields as a Kramers problem,” *Phys. Rev. Lett.* **92**, 250602 (2004).
- [28] B. Mehlig, M. Wilkinson, K. Duncan, T. Weber, and M. Ljunggren, “Aggregation of inertial particles in random flows,” *Phys. Rev. E* **72**, 051104 (2005).
- [29] P. Horvai, “Lyapunov exponent for inertial particles in the 2D Kraichnan mode as a problem Anderson localization with complex valued potential,” preprint nlin.CD/0511023.

- [30] A. Fouxon and P. Horvai “Lyapunov exponent for inertial particles in developed turbulence” (in preparation).
- [31] R.H. Kraichnan, “Small-scale structure of a scalar field convected by turbulence,” *Phys. Fluids* **11**, 945 (1968).
- [32] B.I. Shraiman and E. Siggia, “Scalar turbulence,” *Nature* **405**, 639 (2000).
- [33] G. Falkovich, K. Gawędzki and M. Vergassola, “Particles and fields in fluid turbulence,” *Rev. Mod. Phys.* **73**, 913 (2001).
- [34] V. Oseledets, “A multiplicative ergodic theorem. Characteristic Lyapunov exponents of dynamical systems,” *Trudy Moskov. Mat. Obšč* **19**, 179 (1968).
- [35] G. Paladin and A. Vulpiani, “Anomalous scaling laws in multifractal objects,” *Phys. Rep.* **156** 147 (1987).
- [36] P. Grassberger, “Generalized dimensions of strange attractors,” *Phys. Lett. A* **97**, 227 (1983).
- [37] H.G.E. Hentschel and I. Procaccia, “The infinite number of generalized dimensions of fractals and strange attractors,” *Physica D* **8**, 435 (1983).
- [38] L.-P. Wang, A.S. Wexler, and Y. Zhou, “On the collision rate of small particles in isotropic turbulence. Part I. Zero-inertia case,” *Phys. Fluids* **10**, 266 (1998).
- [39] T.D. Sauer and J.A. Yorke, “Are the dimensions of a set and its image equal under typical smooth functions?” *Ergodic Theory and Dynamical Systems* **17**, 941–956 (1997).
- [40] B. Hunt and V. Kaloshin, “How projections affect the dimension spectrum of fractal measures,” *Nonlinearity* **10**, 1031 (1997).
- [41] N. Sánchez, E.J. Alfaro, and E. Pérez, “The fractal dimension of projected clouds,” preprint astro-ph/0501573.
- [42] L. Biferale, M. Cencini, A. Lanotte, M. Sbragaglia, and F. Toschi, “Anomalous scaling and universality in hydrodynamic systems with power-law forcing,” *New J. Phys.* **6**, 37 (2004); D. Mitra, J. Bec, R. Pandit, and U. Frisch, “Is Multiscaling an Artifact in the Stochastically Forced Burgers Equation?” *Phys. Rev. Lett.* **94**, 194501 (2005).
- [43] M. Wilkinson and B. Mehlig, “Caustics in turbulent aerosols,” *Europhys. Lett.* **71**, 186 (2005).
- [44] A. Keswani and L.R. Collins, “Reynolds number scaling of particle clustering in turbulent aerosols”, *New J. Physics* **6**, 119 (2004).
- [45] J. Bec, “Fractal clustering of inertial particles in random flows,” *Phys. Fluids* **15**, L81 (2003).
- [46] M.R. Maxey, “The gravitational settling of aerosol particles in homogeneous turbulence and random flow fields,” *J. Fluid Mech.* **174**, 441 (1987).

- [47] G. Papanicolaou, “Some probabilistic problems and methods in singular perturbations,” *Rocky Mountain J. Math.* **6** 653–673 (1976).
- [48] W. E, D. Liu and E. Vanden Eijnden, “Analysis of multiscale methods for stochastic differential equations,” *Comm. Pure Appl. Math.* **58**, 1544–1585 (2005).
- [49] U. Frisch, A. Mazzino, A. Noullez, and M. Vergassola “Lagrangian method for multiple correlations in passive scalar advection”, *Phys. Fluids* **11**, 2178 (1999).
- [50] W. Press, S. Teukolsky, W. Vetterling, and B. Flannery, *Numerical Recipes* (Cambridge University Press, Cambridge 1997), Chap. 2.9.